Thin Solid Films 519 (2011) 6092–6096

Contents lists available at ScienceDirect

Thin Solid Films

journal homepage: www.elsevier.com/locate/tsf

The impact of trimethylindium treatment time during growth interruption on the carrier dynamics of InGaN/GaN multiple quantum wells

Shih-Wei Feng [a,*], Hung-Cheng Lin [b], Jen-Inn Chyi [b], Chin-Yi Tsai [a], C.J. Huang [a], Hsiang-Chen Wang [c], Fann-Wei Yang [d], Yen-Sheng Lin [e]

[a] Department of Applied Physics, National University of Kaohsiung, No.700, Kaohsiung University Rd., Nan Tzu Dist., 811. Kaohsiung, Taiwan, ROC
[b] Department of Electrical Engineering, National Central University, Taiwan, ROC
[c] Graduate Institute of Opto-Mechatronics, National Chung Cheng University, Taiwan, ROC
[d] Department of Electronic Engineering, Southern Taiwan University, Taiwan, ROC
[e] Department of Electronic Engineering, I-Shou University, Taiwan, ROC

ARTICLE INFO

Article history:
Received 2 August 2010
Received in revised form 1 April 2011
Accepted 1 April 2011
Available online 9 April 2011

Keywords:
Trimethylindium (TMIn) treatment
Growth interruption
InGaN/GaN
Indium gallium nitride
Gallium nitride
Multiple quantum wells
Carrier dynamic
Photoluminescence

ABSTRACT

Solid-state lighting through light emitting diodes (LEDs) is considered the next generation white-lighting. Because green light affects the quality of white light, significant improvement of the luminescence efficiency of green InGaN LEDs are crucial. In this study, the effects of trimethylindium (TMIn) treatment time during growth interruption on the emission and carrier dynamic characteristics of InGaN/GaN multiple quantum wells with green emission were investigated. TMIn treatment during growth interruption suppresses InGaN decomposition and indium aggregation such that more homogeneous indium composition, higher effective potential level, higher energy (localized) states, stronger photoluminescence (PL) intensity, and an apparent *S*-shaped variation of the temperature-dependent PL peak position were observed. In addition, as the treatment time increases, the decay time and its variation both become smaller. Because indium composition within the InGaN quantum wells is more homogeneous the longer the treatment time, weaker carrier transport and carrier-localized effects lead to a shorter decay time and better recombination efficiency. The research results provide important information to optimize the performance of green and white LEDs.

1. Introduction

Solid-state lighting through light emitting diodes (LEDs) is considered the next generation white-lighting [1,2]. White LEDs can be achieved by color mixing either from the direct output of red, green, and blue LEDs or from color-conversion phosphor [1,2]. Phosphor-based white LEDs with InGaN blue LEDs can achieve external quantum efficiency above 70% [1–4]. Due to the lack of green and red LEDs, the color rendering index of the phosphor-based configuration is relatively low. Because the human eye is most sensitive to green light, green light strongly affects the human perception of the quality of white light. Unfortunately, the quantum efficiencies of both InGaN- and AlInGaP-based LEDs are significantly lower in the green–yellow (500–580 nm) spectral range. This efficiency gap is known as the "green–yellow gap" [1–4]. Because AlInGaP alloy in this spectral range is an indirect bandgap material, a significant improvement of the luminescence efficiency of green and yellow InGaN LEDs is crucial.

InGaN alloys at a high indium mole fraction often lead to a low crystalline quality because of indium aggregation or phase separation [5–7]. Spinodal decomposition produces quantum-dot-like structures which form spatial potential fluctuations and localized states for trapping carriers [5–7]. It is claimed that the electroluminescence emissions come from the recombination of localized excitons in In-rich InGaN clusters [8–12]. In addition, threading dislocations (TDs) and stacking faults (SFs) are commonly observed in GaN-related compounds grown on sapphire. A TD or a SF usually terminates on the sample surface with a V-shaped defect [13–15]. The V-shaped defects are easily formed in the high-indium-content InGaN/GaN multiple quantum wells (MQWs) and triggered by TDs in the buffer layer [13–15]. These defects are formed because of strain relaxation associated with stacking faults or indium aggregation [16–18].

It was shown that the quality of InGaN/GaN MQWs was improved by reducing the density of V-shaped defects through the growth interruption technique [19,20]. By introducing growth interruption at high growth temperature, atoms can relax into the minimum energy sites to approach thermal equilibrium. Due to the thermal annealing effect, strain relaxation and indium desorption lead to decomposition of In-rich InGaN such that a flat InGaN surface and better InGaN/GaN quantum well structure were obtained. Hence, better quality of the InGaN layer and reduced defect density enhance the luminescence intensity [19,20]. Also, another growth interruption technique was proposed in our previous study [21]. During the growth interruption at each InGaN-well-

* Corresponding author. Tel.: +886 7 5919470; fax: +886 7 5919357.
E-mail address: swfeng@nuk.edu.tw (S.-W. Feng).

0040-6090/$ – see front matter © 2011 Elsevier B.V. All rights reserved.
doi:10.1016/j.tsf.2011.04.004

to-GaN-barrier interface, only trimethylindium (TMIn) and NH_3 were allowed to flow into the reactor. This is called "TMIn treatment". By using TMIn treatment during the growth interruption, the reduced V-shaped defect density and surface smoothing process due to ambient TMIn result in a better InGaN/GaN quantum well structure. Hence, the internal quantum efficiency and output power of InGaN/GaN green LEDs are enhanced [21]. However, the impact of TMIn treatment time during growth interruption on the carrier dynamics of InGaN/GaN multiple quantum wells was not well studied.

In this study, the effects of TMIn treatment time during growth interruption on the emission and carrier dynamic characteristics of InGaN/GaN MQWs with green emission were investigated. With TMIn treatment, more homogeneous indium composition, higher effective potential level, higher energy (localized) states, stronger photoluminescence (PL) intensity, and an apparent *S*-shaped variation of the temperature-dependent PL peak position were observed. Because the indium composition within the InGaN quantum wells is more homogeneous the longer the treatment time in the TMIn-treated samples, weaker carrier transport and carrier-localized effects lead to shorter decay times and better recombination efficiency.

This paper is organized as follows: in Section 2, sample structures and experimental procedures are described. In Section 3, experimental results and discussion are reported. Finally, conclusions are drawn in Section 4.

2. Sample structures and experimental procedures

To study the effects of TMIn treatment during the growth interruption at each InGaN-well-to-GaN-barrier interface, four samples were grown on *c*-sapphire by low-pressure metal organic vapor phase epitaxy. The sample structures consist of a 30 nm GaN nucleation layer, a 1.5 μm GaN buffer layer, a 2.5 μm *n*-type GaN contact layer, and five GaN(15 nm)/InGaN(3 nm) MQWs. The substrate temperatures for the low-temperature GaN nucleation layer and high temperature GaN buffer layer were 530 and 1100 °C, respectively. The MQWs were grown at 780 °C. At each InGaN-well-to-GaN-barrier interface during the growth interruption, only TMIn and NH_3 were allowed to flow into the reactor. This is called "TMIn treatment". The details of growth procedures were described in the previous study [21]. With the same sample structures, three samples with different TMIn treatment times and one control sample (TMIn-0sec) without TMIn treatment were prepared. TMIn treatment times for the TMIn-60sec, TMIn-120sec, and TMIn-180sec MQW samples were 60, 120, and 180 s, respectively.

Experiments were conducted on all four samples. The structural properties of the samples were investigated by a high-resolution X-ray diffractometer (XRD). The surface morphology was revealed by atomic force microscopy (AFM) (Park Systems, XE-70) with a non-contact mode using a silicon tip of curvature less than 10 nm. PL measurements were carried out with the 325 nm line of a 50 mW He–Cd laser for excitation. For time-resolved photoluminescence (TRPL) measurements, a picosecond diode laser (PicoQuant) generated optical pulses of 100 ps width with a 5 MHz repetition rate to excite the epilayers. The excitation energy (wavelength) was 3.324 eV (375 nm) for pumping the InGaN wells. Light emitted from the sample was detected by a photomultiplier (PMT) and a monochromator. The signal from the PMT was recorded by means of time-correlated single-photon-counting technology (PicoQuant, Model TimeHarp 200). The overall time resolution was 50 ps. The samples were placed in a cryostat for low-temperature measurements.

3. Results and discussion

3.1. XRD and AFM results

Fig. 1 shows the XRD patterns for the four samples. The diffraction peaks corresponding to GaN, InGaN, and InN can be identified [5]. The

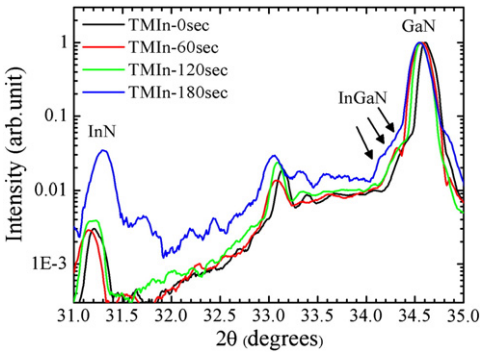

Fig. 1. XRD patterns for the TMIn-0sec, TMIn-60sec, TMIn-120sec, and TMIn-180sec samples.

GaN diffraction peak is mainly from the contact and barrier layers. The side shoulder with a broad distribution below the GaN main peak is attributed to InGaN with various indium contents, sizes, and shapes in the quantum wells. This suggests indium aggregation in the quantum well region. With a longer treatment time (except for the TMIn-180sec sample), a narrower width and a slightly decreasing position of GaN diffraction peak with a smaller side shoulder are observed. Because indium diffusion into the barrier region in the TMIn-treated samples is suppressed, a better quantum well structure is observed. The indium composition in the well region becomes homogeneous. A slightly decreasing position of the GaN main peak implies strain relaxation inside the quantum well region. For the TMIn-180sec sample, due to the solubility limit of indium in GaN, the suppressed diffusion of indium atoms leads to a decomposed phase consisting of InN and slightly broad InGaN distribution. Slight phase separation and indium aggregation reoccur. The weak peak around 33° represents InGaN with 30–35% indium content in the well region.

Fig. 2 shows the surface morphologies of the four samples as revealed by AFM. With TMIn treatment, the surface morphologies of the TMIn-60sec and TMIn-120sec samples become smooth and the density of V-shaped defects decreases. The postulate that TMIn treatment improves material quality and enhances the internal quantum efficiency and output power of InGaN/GaN green LEDs is confirmed. For the TMIn-180sec sample, slight phase separation and indium aggregation result in a little rough surface morphology.

3.2. PL results

Fig. 3(a) shows the PL spectra as functions of temperature for the TMIn-0sec sample. UV and green emission bands were both observed for the four samples (Fig. 3(b)). The UV band was attributed to *p*-GaN while the green band comes from the InGaN/GaN MQWs [22]. Due to nonradiative recombination, the intensities of PL spectra show a decreasing trend at higher temperature(s). In addition, Fig. 3(b) shows normalized PL spectra of the four samples at 10 K. As TMIn treatment time increases, the spectrum shows a slightly blue-shifted peak position. By using TMIn treatment during the growth interruption, the annealing effect leads to more homogeneous indium composition inside the quantum wells so that the effective potential level in the quantum well becomes more homogeneous and slightly higher. Hence, as TMIn treatment time increases, the peak position is slightly blue-shifted.

Fig. 4(a) shows the integral intensity as a function of temperature for the four samples. The integral intensities of UV emission for the four samples are nearly equal, while with a longer TMIn treatment time, a larger integral intensity of green emission is observed. Due to the same *p*-*i*-*n* device structure, the *p*-GaN layer is presumed to contribute the same intensity of UV emission. The stronger integral intensity of green emission for the TMIn-treated samples suggests better quantum well structures and a reduced V-shaped defect

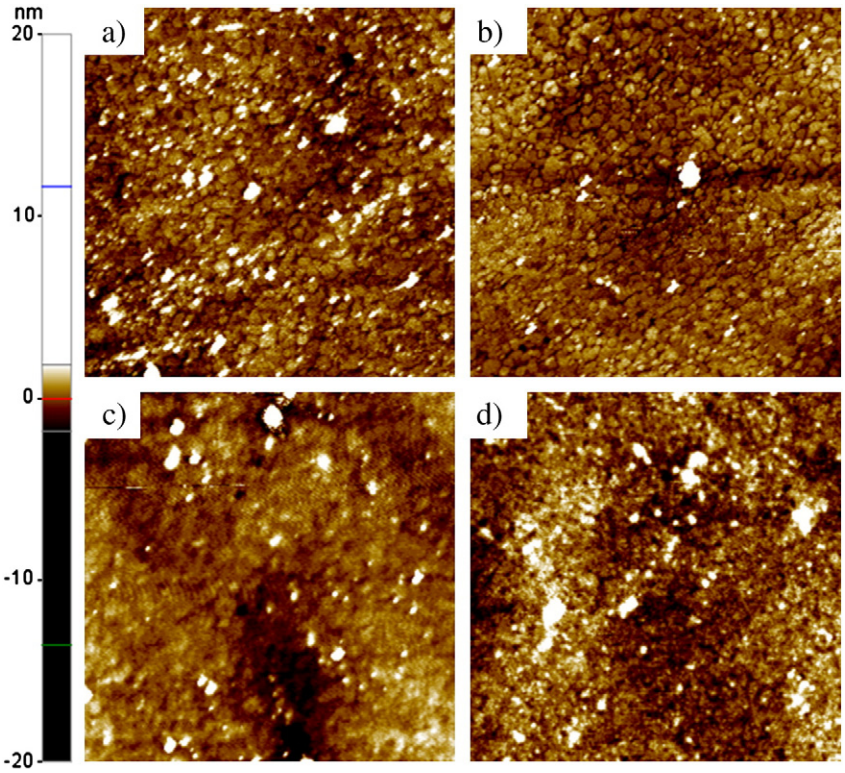

Fig. 2. AFM images (2 × 2 μm) of the (a) TMIn-0sec, (b) TMIn-60sec, (c) TMIn-120sec, and (d) TMIn-180sec samples with surface roughness: 0.608, 0.530, 0.522, and 0.576 nm, respectively.

density. Although slight phase separation, indium aggregation, and slightly rough surface morphology of the TMIn-180sec sample may degrade the sample quality, a lower V-shaped defect density leads to its generating a stronger PL intensity [21]. In addition, Fig. 4(b) shows green peak position as a function of temperature. The temperature variations of the PL peaks of the four samples show a red-blue-red-shift variation with increasing temperature, i.e., "*S*-shaped" behavior. The blue-shift behavior is due to the recombination of excitons receiving thermal energy within carrier localization in potential minimums [11,23,24]. The blue-shift continues with increasing temperature until localized carriers overcome the potential barrier to become free carriers. It is observed that the longer the treatment time, the more apparent the blue-shift. The apparent blue-shift in the TMIn-180sec sample is attributed to the slight phase separation and indium aggregation. Such blue-shift is also attributed to the shorter

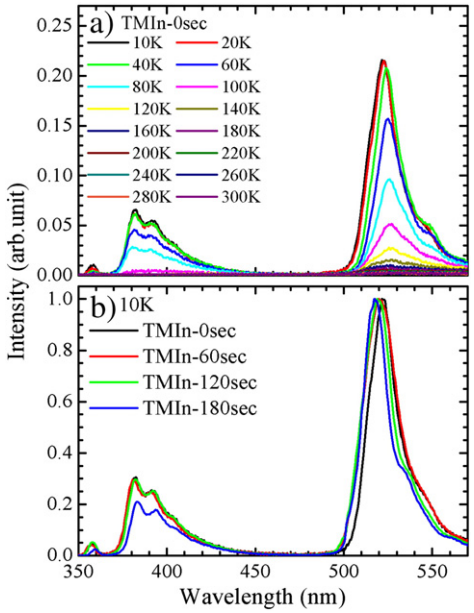

Fig. 3. (a) PL spectra as functions of temperature for the TMIn-0sec sample; (b) normalized PL spectra at 10 K for the four samples.

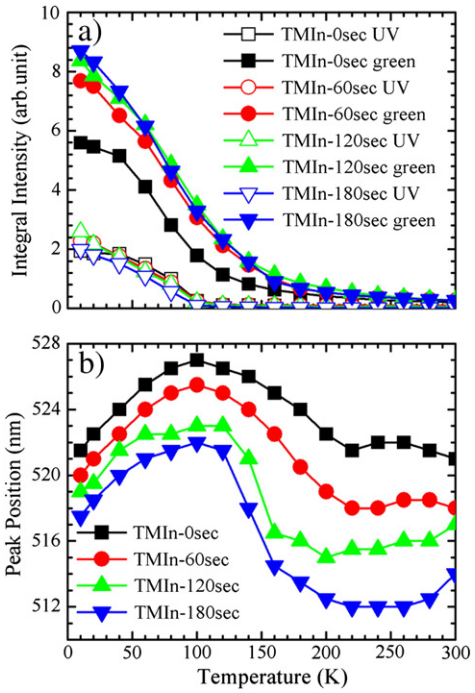

Fig. 4. (a) Integral intensity and (b) peak position of green band as functions of temperature for the four samples.

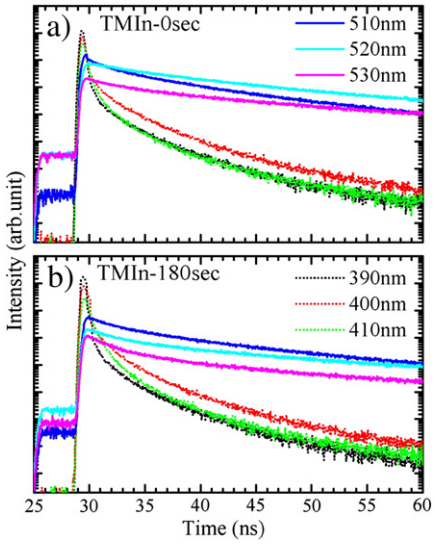

Fig. 5. TRPL decay profiles at 10 K for the (a) TMIn-0sec and (b) TMIn-180sec samples.

carrier lifetime. Due to the increasing dissociation rate and non-radiative processes in the temperature range from 120 K to 220 K, the decreasing carrier lifetime leads to carrier recombination in the higher energy states before reaching the lower energy tail states [23]. As shown in Fig. 6, the shorter carrier lifetime of a TMIn-treated sample enhances carrier recombination on the higher energy side and leads to an apparent blue-shift of the PL peak energy.

3.3. TRPL results

Fig. 5(a) and (b) shows TRPL decay profiles at 10 K for the TMIn-0sec and TMIn-180sec samples, respectively. The temporal profiles can be categorized into two groups: UV (dotted lines) and green (solid lines) emission bands. The profiles of UV emissions decay fast while those of green emissions decay slowly. Because the larger indium composition fluctuation in the active region enhances the localization effect, green emission is favored by the localized exciton model. In addition, decay profiles of both UV and green bands exhibit nonexponential decay. Nonexponential decay associated with recombination dynamics was described by recombination models [25–28]. In our previous study, the mechanism of carrier transport among different levels of localized states in indium-rich clusters was proposed to explain the early-stage fast decay, delayed slow rise, and extended slow decay of TRPL intensity [11]. Because of the existence of the delayed slow rise, early-stage fast decay, and extended slow decay in the decay profiles, the carrier transport model was adopted to analyze the recombination dynamics. The decay profiles were fitted with double exponential decays to trace out the early-stage (fast) and extended (slow) decay times. Because the early-stage (fast) amplitude fractions for all PL decay profiles are over 80%, the discussion focuses on the early-stage decay times.

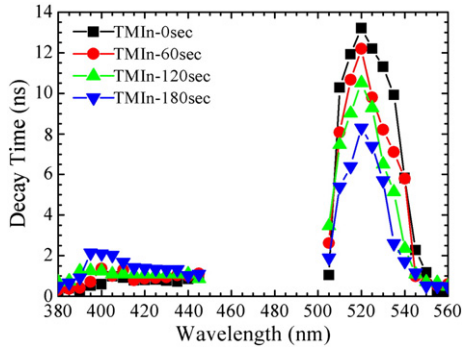

Fig. 6. TRPL decay times at 10 K for the four samples.

Fig. 6 shows TRPL decay times at 10 K for the four samples. For both UV and green bands, the decay time increases first and then decreases with increasing emission wavelength. The increasing trend of the left-hand side of the green peak of the decay times is due to weaker carrier capture of relatively shallower localized states and/or partially due to faster recombination in weakly localized states. Because carrier transport into strongly localized states requires a certain energy to overcome a potential barrier, it is more difficult for carriers to transfer into strongly localized states. This leads to the shorter decay times on the low energy ends of spectra. In our previous study, the mechanism of carrier transport among different levels of localized states in indium-rich clusters was proposed to explain this characteristic of decay time [11]. In addition, the localized exciton model, whose trap centers originate from a spatial disorder such as the fluctuation of the well width and/or the In composition fluctuation within InGaN/GaN MQWs, was also proposed to explain this characteristic of decay time [29,30]. Within the localization model, strongly localized (lower-energy) excitons decay primarily via radiative recombination, while weakly localized (higher-energy) excitons exhibit a decreased decay time due to the additional channel of transfer to lower-energy sites [29,30]. Furthermore, the variation of decay time for the green band is larger than that for the UV band. Because the green band comes from the InGaN/GaN MQWs, carrier transport and carrier localization effects of the green band are expected. As the TMIn treatment time increases, the decay time and its variation in the green band both become smaller. Because TMIn treatment leads to more homogeneous indium composition within the InGaN quantum wells, weaker carrier transport and carrier-localized effects lead to shorter decay times and small variations. It is noted that the radiative recombination is dominant at the low temperature. Hence, TMIn treatment results in shorter radiative decay times and enhances the recombination efficiency.

4. Conclusions

In summary, we have studied the effects of TMIn treatment on the emission and carrier dynamic characteristics of InGaN/GaN MQWs with green emission. With TMIn treatment, more homogeneous indium composition, higher energy (localized) states, stronger PL intensity, and an apparent *S*-shaped variation of the temperature-dependent PL peak position were observed. Because the indium composition within the InGaN quantum wells is more homogeneous the longer the treatment time, weaker carrier transport and carrier-localized effects lead to shorter decay times and better recombination efficiency. The research results can be used to optimize the performance of green and white LEDs.

Acknowledgment

This research was supported by the National Science Council, Taiwan, ROC, under grants NSC 98-3114-E-110-001, NSC 99-2112-M-390-002-MY3, and NSC 99-2515-S-390-001.

References

[1] E. Fred Schubert, Light-Emitting Diodes, 2006 Cambridge.
[2] The Optoelectronics Industry Development Association (OIDA), http://www.oida.org.
[3] M.R. Krames, O.B. Shchekin, R. Mueller-Mach, G.O. Mueller, L. Zhou, G. Harbers, M. George Craford, J. Disp. Technol. 3 (2007) 160.
[4] J.M. Phillips, M.E. Coltrin, M.H. Crawford, A.J. Fischer, M.R. Krames, R. Mueller-Mach, G.O. Mueller, Y. Ohno, L.E.S. Rohwer, J.A. Simmons, J.Y. Tsao, Laser Photonics Rev. 1 (2007) 307.

[5] Y.S. Lin, K.J. Ma, C. Hsu, S.W. Feng, Y.C. Cheng, C.C. Liao, C.C. Yang, C.C. Chou, C.M. Lee, J.I. Chyi, Appl. Phys. Lett. 77 (2000) 2988.
[6] S.F. Chichibu, A. Uedono, T. Onuma, B.A. Haskell, A. Chakraborty, T. Koyama, P.T. Feni, S. Keller, S.P. Denbaars, J.S. Speck, U.K. Mishra, S. Nakamura, S. Yamaguchi, S. Kamiyama, H. Amano, I. Akasaki, J. Han, T. Sota, Nat. Mater. 5 (2006) 810.
[7] Y. Narukawa, Y. Kawakami, M. Funato, Sz. Fujita, S. Fujita, S. Nakamura, Appl. Phys. Lett. 70 (1997) 981.
[8] Y. Narukawa, Y. Kawakami, S. Fujita, S. Fujita, S. Nakamura, Phys. Rev. B 55 (1997) R1938.
[9] S.F. Chichibu, K. Wada, J. Müllhäuser, O. Brandt, K.H. Ploog, T. Mizutani, A. Setoguchi, R. Nakai, M. Sugiyama, H. Nakanishi, K. Korii, T. Deguchi, T. Sota, S. Nakamura, Appl. Phys. Lett. 76 (2000) 1671.
[10] Y. Narukawa, Y. Kawakami, S. Fujita, S. Nakamura, Phys. Rev. B 59 (1999) 10283.
[11] S.W. Feng, Y.C. Cheng, Y.Y. Chung, C.C. Yang, Y.S. Lin, C. Hsu, K.J. Ma, J.I. Chyi, J. Appl. Phys. 92 (2002) 4441.
[12] S.W. Feng, T.Y. Tang, Y.C. Lu, S.J. Liu, E.C. Lin, C.C. Yang, K.J. Ma, C.H. Shen, L.C. Chen, K.H. Kim, J.Y. Lin, H.X. Jiang, J. Appl. Phys. 95 (2004) 5388.
[13] X.H. Wu, C.R. Elsass, A. Abare, M. Mack, S. Keller, P.M. Petroff, S.P. DenBaars, J.S. Speck, S.J. Rosner, Appl. Phys. Lett. 72 (1998) 692.
[14] H.K. Cho, J.Y. Lee, G.M. Yang, C.S. Kim, Appl. Phys. Lett. 79 (2001) 215.
[15] N. Sharma, P. Thomas, D. Tricker, C. Humphreys, Appl. Phys. Lett. 77 (2000) 1274.
[16] C.J. Sun, M. Zubair Anwar, Q. Chen, J.W. Yang, M. Asif Khan, M.S. Shur, A.D. Bykhovski, Z. Liliental-Weber, C. Kisielowski, M. Smith, J.Y. Lin, H.X. Xiang, Appl. Phys. Lett. 70 (1997) 2978.
[17] I.H. Kim, H.S. Park, Y.J. Park, T. Kim, Appl. Phys. Lett. 73 (1998) 1634.
[18] Y. Chen, T. Takeuchi, H. Amano, I. Akasaki, N. Yamada, Y. Kaneko, S.Y. Wang, Appl. Phys. Lett. 72 (1998) 710.
[19] H.K. Cho, J.Y. Lee, N. Sharma, J. Humphreys, G.M. Yang, C.S. Kim, Phys. Status Solidi B 228 (2001) 165.
[20] N.H. Niu, H.B. Wang, J.P. Liu, N.X. Liu, Y.H. Xing, J. Han, J. Deng, G.D. Shen, Optoelectron. Lett. 3 (2007) 15.
[21] H.C. Lin, R.S. Lin, J.I. Chyi, Appl. Phys. Lett. 92 (2008) 161113.
[22] E. Oh, H. Park, Y. Park, Appl. Phys. Lett. 72 (1998) 70.
[23] Y.H. Cho, G.H. Gainer, A.J. Fischer, J.J. Song, S. Keller, U.K. Mishra, S.P. DenBarrs, Appl. Phys. Lett. 73 (1998) 1370.
[24] P.G. Eliseev, P. Perlin, J. Lee, M. Osinski, Appl. Phys. Lett. 71 (1997) 569.
[25] H. Scher, M. Shlesinger, J. Bender, Phys. Today 44 (1) (1991) 26.
[26] T. Bartel, M. Dworzak, M. Strassburg, A. Hoffmann, A. Strittmatter, D. Bimberg, Appl. Phys. Lett. 85 (2004) 1946.
[27] P. Lefebvre, S. Kalliakos, T. Bretagnon, P. Valvin, T. Taliercio, B. Gil, N. Grandjean, J. Massies, Phys. Rev. B 69 (2004) 035307.
[28] A. Morel, P. Lefebvre, S. Kalliakos, T. Taliercio, T. Bretagnon, B. Gil, Phys. Rev. B 68 (2003) 045331.
[29] H.S. Kim, R.A. Mair, J. Li, J.Y. Lin, H.X. Jiang, Appl. Phys. Lett. 76 (2000) 1252.
[30] Y. Narukawa, Y. Kawakami, S. Fujita, S. Fujita, S. Nakamura, Phys. Rev. B 55 (1997) R1938.